Supporting Information

Synergistic Effect of Au-PdO Modified Cu-doped $K_2W_4O_{13}$ Nanowires for Dual Selectivity High Performance Gas Sensing

Shah Zeb,[a,b,c] Yu Cui,[c] Heng Zhao,[c] Ying Sui,[c] Zhen Yang,[c] Zia Ullah Khan,[d] Shah Masood Ahmad,[d] Muhammad Ikram,[a,b] Yongxiang Gao,[a] and Xuchuan Jiang[c*]*

[a]Institute for Advanced Study, Shenzhen University, Nanhai Avenue 3688, Shenzhen518060, PR China.

[b]College of Physics and Optoelectronic Engineering, Shenzhen University, Shenzhen 518060, PR China.

[c]School of Chemistry and Chemical Engineering, Institute for Smart Materials and Engineering, University of Jinan, No. 336 Nanxinzhuang West Road, 250022, Jinan, PR China.

[d]National Centre of Excellence in Physical Chemistry, University of Peshawar, Peshawar 25120, Pakistan

Corresponding Author

* Y. Gao (E-mail: yongxiang.gao@szu.edu.cn) * X. Jiang (E-mail: ism_jiangxc@ujn.edu.cn)

S1. MATERIALS

Sodium tungstate dihydrate ($Na_2WO_4 \cdot 2H_2O$, 99.5%), palladium (II) chloride ($PdCl_2$ (≥99.9%) Sigma Aldrich), hydrogen tetrachloroaurate (III) trihydrate ($HAuCl_4 \cdot 3H_2O$ (≥99.9%) Sigma Aldrich), potassium sulfate (K_2SO_4, 99%), copper (II) chloride dehydrate ($CuCl_2.2H_2O$), nickel chloride ($NiCl_2$), ferric chloride hexahydrate ($FeCl_3.6H_2O$), hydrochloric acid (HCl, 37%), ethanol absolute (C_2H_5OH, 99.8%) were purchased from Macklin, and used. All solutions were carefully prepared in deionized-distilled water (DDI), and during experiments, glassware (Pyrex) was properly washed with aqua regia.

S2. Synthesis of Doped $K_2W_4O_{13}$ Nanowires

Cu-doped $K_2W_4O_{13}$ nanowires were synthesized by hydrothermal method, as follows "1.65 g of $Na_2WO_4 \cdot 2H_2O$ was dissolved in 40 mL of distilled water-ethanol mixtures, and the water/ethanol volume ratio was kept 7:1. Then, a 3 M HCl aqueous solution was added dropwise to the tungsten solution under continuous stirring until pH to 2. After that, different amounts of $CuCl_2 \cdot 2H_2O$ (1.0 wt%, 2.0 wt%, and 3.0 wt%, Cu/W) were added (**Table S1**) into the W-precursor solution. 2.6 g of K_2SO_4 was mixed into the above clear solution and stirred for 30 min. The white turbid solution was then poured slowly into the

Teflon-lined stainless-steel autoclave for hydrothermal treatment at 180 °C for 20 h. Finally, Cu-doped $K_2W_4O_{13}$ samples (WOC) were collected by centrifugation and dried at 60 °C. Similar procedures were carried for Ni-doped $K_2W_4O_{13}$ and Fe-doped $K_2W_4O_{13}$, instead of without $NiCl_2$ and ferric chloride ($FeCl_3.6H_2O$) as resources of Ni and Fe, and either of them. Water/Ethanol co-solvent volume ratio (40:0, 19:1, 7:1, 3:1, & 1:1) was adjusted by varying the volume of ethanol, keeping the total volume at 40 mL.

S3. Preparation of AuPdO Modified Cu-doped $K_2W_4O_{13}$ Nanowires

The PdO, Au, and Au-PdO nanoparticles were decorated onto the WOC by impregnation[1] and *in-situ* reduction[2]. The first step was to prepare PdO decorated WOC;100 mg of WOC sample was dispersed in 10 mL of ethanol and stirred for an hour, then 240 µL $PdCl_2$ (0.05 M) was dropped, and the resultant suspension quaked for 8 h. Thus, PdO-WOC composite (0.96wt%) was recovered after washing and drying, named PWOC. Similarly, 0.05 to 0.5wt% PdO decorated WOC were also prepared by variation of $PdCl_2$ solution in the range of 80-480 µL. The ultrathin $K_2W_4O_{13}$ nanowires have high surface energy, which is further improved by Cu-doping. Ethanol solvent provides weak reducing media, leading to the formation of PdO-WOC nanocomposites.

The Au nanoparticles were also loaded in which 80 µl of $HAuCl_4{\cdot}3H_2O$ solution (0.05 M) was dropped into a water suspension containing 80 mg of well-dispersed PdO-WOC sample. 200 µL of $NaBH_4$ (0.05 M) drop-wise added and then quaked for 6 h. The product Au-PWOC with

(0.96wt% Pd & 2.40wt% Au) was collected. Finally, the recovered 3wt% Au-PWOC samples named APWOC were then kept to calcination at 380 ˚C for 4 h. For comparison, sample 1.5wt% and 5wt% APWOC samples were also prepared in which the $HAuCl_4 \cdot 3H_2O$ solution concentrations varied from 80-360 μL.

S4. Materials Characterization

The shape and size of the sensor samples were studied by field emission scanning electron microscope (FESEM, Quanta FEG250, facilitated with energy-dispersive X-ray spectroscopy (EDS), transmission electron microscope (TEM, JEOL, JEM-1400), and high–resolution TEM (HRTEM, JEOL 2100 F). The X-ray photoelectron spectroscopy (XPS) was studied by SmartLabSE, Rigaku with the Cu Kα, $h\nu$=284.6 eV. The composition and samples crystallinity were studied by X-ray diffraction spectroscopy (XRD, SmartLabSE, Rigaku) with Cu-Kα radiation (λ = 1.5418 Å). Nitrogen adsorption and desorption processes were studied by Kubu X1000. The Brunauer–Emmett–Teller (BET) and Barrett–Joyner–Halenda (BJH) schemes were used to measure the specific surface area (S_{BET}) and the pore size distribution. Before BET experiments, sample batches were properly heated under vacuum at 200 ˚C for 6 h. UV–vis diffuse reflection spectroscopy (DRS) was obtained on a Shimadzu UV-3600 spectrophotometer

in $BaSO_4$ as a reference standard.

S5. Sensing Measurements

The sensing properties of the fabricated sensors were examined with CGS-MT Mini, Multi-functional Probe Station (Beijing Sino Aggtech Co. Ltd., China), following a static gas-sensing procedure.[2] A proper amount of pristine, doped, and surface-modified samples were mixed with ethanol which was then drop-casted on the Ag-Pd printed alumina substrate with a microsyringe to form a thin layer as the sensor material. After coating, the sensors were dried at 60 °C on a heating plate, followed by sintering for 2 h at elevated temperature of 200 °C in the sealed chamber of the sensor system to remove aqueous impurities. During the measurements, the fabricated sensors were heated to the working temperatures ranging from 50 to 300 °C to achieve a stable resistance in air (R_a). The volume of liquids for testing target gases was measured in microliters (μL) and was injected through a microsyringe into the test chamber for gas detection. The following formula was used to calculate the concentration of gas;

$$Q=(V\times C\times M)/(22.4\times d\times \rho)\times 10^{-6}\times(273+T_R)/(273+T_B) \quad (1)$$

Where,

Q is the volume of the liquid to be taken (μL); V is the volume of the test bottle (mL); M is the molecular weight of the substance (g); d is the purity of the liquid; C is the concentration of the

gas to be formulated (ppm); ρ is the density of the liquid (g/cm^3); T_R is the test ambient temperature (°C); T_B is the temperature inside the test bottle (°C).

Here, liquid 3H-2B, TEA and some other VOCs were injected through a microsyringe into the testing chamber and heated above their boiling points for the preparation of gases, which led to a new steady resistance, known as sensor`s resistance in the test gas (R_g). The NH_3 gas tested in this work is wet due to trace water. To investigate the effect of H_2O molecules during the NH_3 sensing, control experiments of pure water were conducted and we found negligible influence under the reported conditions. The sensitivity of the sensors was assessed by the parameter $S=R_a/R_g$. All the gas sensing measurements were conducted in a clean room at 25 °C and a relative humidity (RH) of 18%. After optimization, the operating temperature was set to 120 °C for 3H-2B and 200 °C for TEA at a controlled RH value of 12%.

Table S1 Preparation of different contents of Cu-$K_2W_4O_{13}$ materials;

Sensor materials	$Na_2WO_4 \cdot 2H_2O$ (mg)	$CuCl_2 \cdot 2H_2O$ (mg)	Water/Ethanol (7:1 Volume)	K_2SO_4 (mg)	Temperature (ºC)	Time (h)
$K_2W_4O_{13}$	1.65	0				
1% Cu-$K_2W_4O_{13}$	1.65	0.007				
2%Cu-$K_2W_4O_{13}$	1.65	0.017	35 mL+5 mL	2.6	180	20
3% Cu-$K_2W_4O_{13}$	1.65	0.025				

Table S2. Preparation parameters of PdO modified Cu-doped $K_2W_4O_{13}$ composite

Samples	WOC (mg)	H_2O (mL)	$PdCl_2$ (μL)	$NaBH_4$ (0.05 M)	Pd ICP (Wt%)	Pd Wt%
2 wt% Cu doped $K_2W_4O_{13}$	60	20	-		-	
0.05 wt% Pd-WO_3	60	20	80	50	0.053	0.12
0.5 wt% Pd-WO_3	60	20	160	50	0.09	0.26
1 wt% Pd-WO_3	60	20	240	50	0.198	0.96

Table S3. Preparation parameters of Au modified Cu–doped $K_2W_4O_{13}$ composite

Samples	WOC (mg)	H_2O (mL)	$HAuCl_4$ (μL)	$NaBH_4$ (0.05 M)	Au ICP (Wt%)	Au Wt%
2 wt% Cu doped $K_2W_4O_{13}$	60	20	-		-	
0.05 wt% Pd-WO_3	60	20	80	150	0.197	0.12
0.5 wt% Pd-WO_3	60	20	120	350	0.28	2.26
1 wt% Pd-WO_3	60	20	240	350	0.465	4.96

Table S4. Preparation parameters of bimetals Au-PdO modified Cu–doped $K_2W_4O_{13}$ composites

Samples	1 wt.% PdO-WOC (mg)	H_2O (mL)	$HAuCl_4$ (μL)	(0.05 M) $NaBH_4$ (μL)	ICP Wt% Au	Wt % Au
2 wt% AuPd-WO_3	50	20	40	150	0.129	1.56
3 wt% AuPd-WO_3	50	20	80	300	0.224	2.40
5 wt% AuPd-WO_3	50	20	160	450	0.455	4.12

S6. XRD, Optical Absorption and BET Surface Area Analysis

The as-prepared $K_2W_4O_{13}$, doped WOC, WON, WOF, and surface decorated samples, i.e., PWOC and APWOC were investigated by XRD as shown in **Figure 3a**. The pure $K_2W_4O_{13}$ sample (Figure 1a) indexed typical hexagonal $K_2W_4O_{13}$ (JCPDS # 20-0942) with preferential crystal growth at <001> and <002> planes, corresponding to substructure reported for nonstoichiometric WO_{3-x} and consistent with our reported work.[3] No obvious peaks and phase change of tungsten oxide was detected because of the low impurity Cu/Fe doping atoms **(Figure 3aii,iii)**; however, WON produced certain peaks as shown in **Figure 3iv.** Compared to $K_2W_4O_{13}$ the diffraction peaks of WOC, WOF, and WON samples show a slight shift to a high angle, suggesting the successful incorporation of impurity atoms into the lattice of tungsten oxide. Furthermore, the XRD patterns of PWOC and APWOC hybrid composite samples calcined at 380 °C for 4 h are shown in **Figure 3v,vi.** There is no obvious Pd/PdO nanoparticles peak on the WOC sample; because the PdO has low-density distribution and small atomic size, making peak strength indiscernible. The Au-PdO nanoparticles loaded to the WOC appeared wide diffraction peaks at 28.28° and 44.54°, correspond to <111> and <200> planes, describe the gold nanoparticles in (JCPDS # 04–0784) as shown in **Figure 3vi**. The PdO and Au contents were analyzed by EDS elemental mapping and ICP-AES experiments which highlighted the actual amount of PdO and Au on the PWOC and Au-PdO-WOC nanowires, which were closer to the theoretical values.

The UV−vis DRS spectra of the doped and surface modified samples are shown in **Figure 3b.** The smooth absorption curves with no observable hump demonstrate the homogeneous incorporation of metals into the $K_2W_4O_{13}$ lattices, consistent with the XRD results. Moreover, the WOC, WON, and WOF have lowered absorptivity in the visible region (500−700 nm)

compared to $K_2W_4O_{13}$. The intrinsic absorptivity of the WOC sample was maintained with the loading of PdO, Au, and Au-PdO nanoparticles, and the absorption edge is extended toward a higher wavelength. Moreover, due to the LSPR effect of Au nanoparticles, a new band appears around 450-650 nm, particularly for the AWOC sample. The bandgap energy (E_g) was estimated from the equation, $(\propto h\nu)^{1/2} = A(h\nu - Eg)$, where h is the Planck's constant ($1.69x10^{-19}$), ν is the light frequency, A is the dimensional constant, α is the absorption coefficient, and n is for direct/indirect transition. The estimated E_g values are 2.98, 2.73, 2.83, 2.75, 2.6, 2.61, and 2.5 eV for $K_2W_4O_{13}$, WOC, WOF, WON, AWOC, PWOC, and APWOC, respectively. Thus, it can be seen that metal incorporation gradually reduces the bandgap energy of tungsten oxide. The oxidation reaction and growth of PdO/Au nanoparticles occur on the surface of WOC. Either surface decoration/fusion of the Cu, PdO, and AuPdO atoms can substitute the W atoms and may occupy the surface lattice sites, thus changing the bandgap energy, specific surface area, and conductivity of the material.[2] The specific surface area (S_{BET}) of doped and loaded samples is provided in **Figure S2.** The S_{BET} derived for WOC, WON, WOF, PWOC, AWOC and APWOC are 70.218, 62.417, 58.757, 72.423, 78.725 and 70.641 m^2/g, respectively. The S_{BET} of doped nanostructures is higher than that of WO_3 previously reported.[3, 4] The pore size is around 10 nm, demonstrating the mesoporous nature of the particles. Moreover, Pd/PdO, Au, and AuPdO loadings can further increase the surface area. It is noteworthy that loadings of larger-sized noble metals have decreased the $S_{BET,}$ which may be due to the nanoparticle agglomeration.[1] Generally, the increased S_{BET} is highly conducive in gas sensing performance.

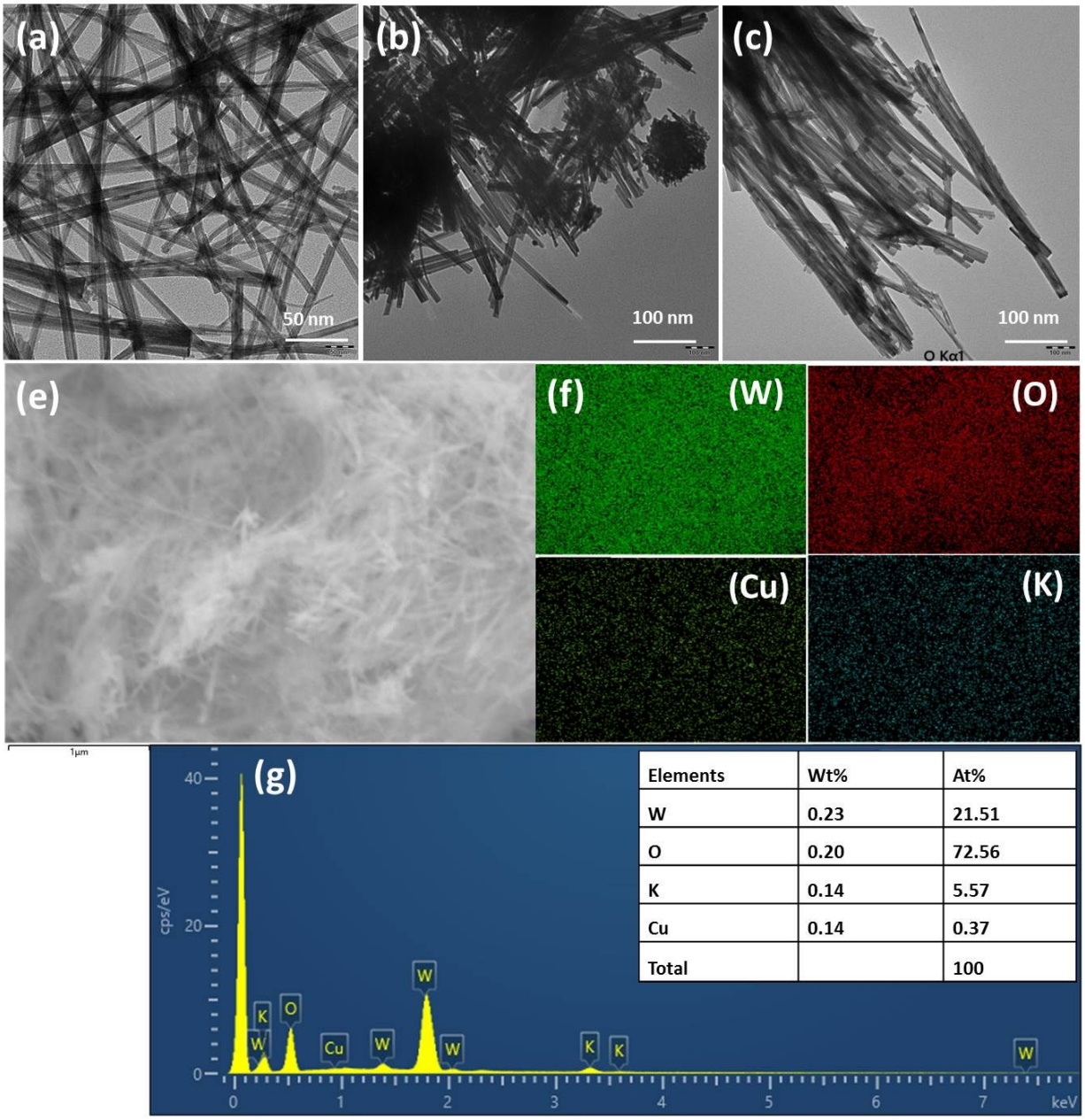

Figure S1. TEM image of (a) pristine $K_2W_4O_{13}$,(b) Ni-doped $K_2W_4O_{13}$, (c) Fe-doped $K_2W_4O_{13}$, (d-g) EDS elemental mapping of Cu-doped $K_2W_4O_{13}$ sample showing the distribution of elements.

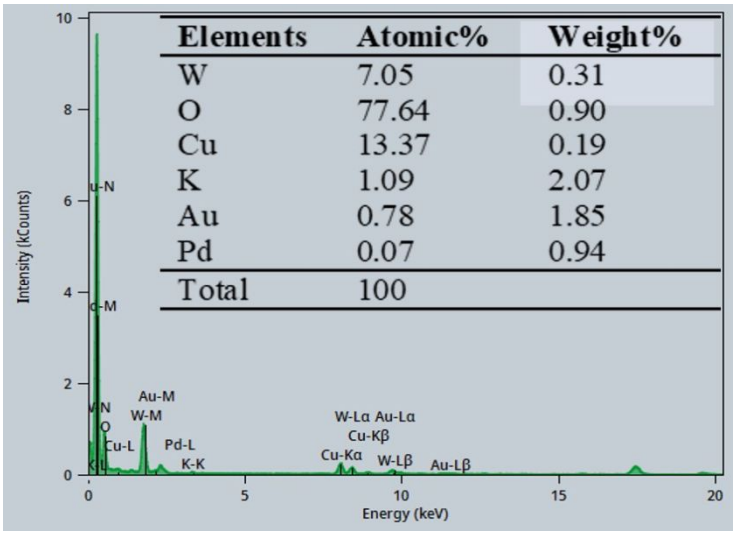

Figure S2. EDS elemental mapping showing the distribution of W, O, Cu, K, Pd, and Au elements

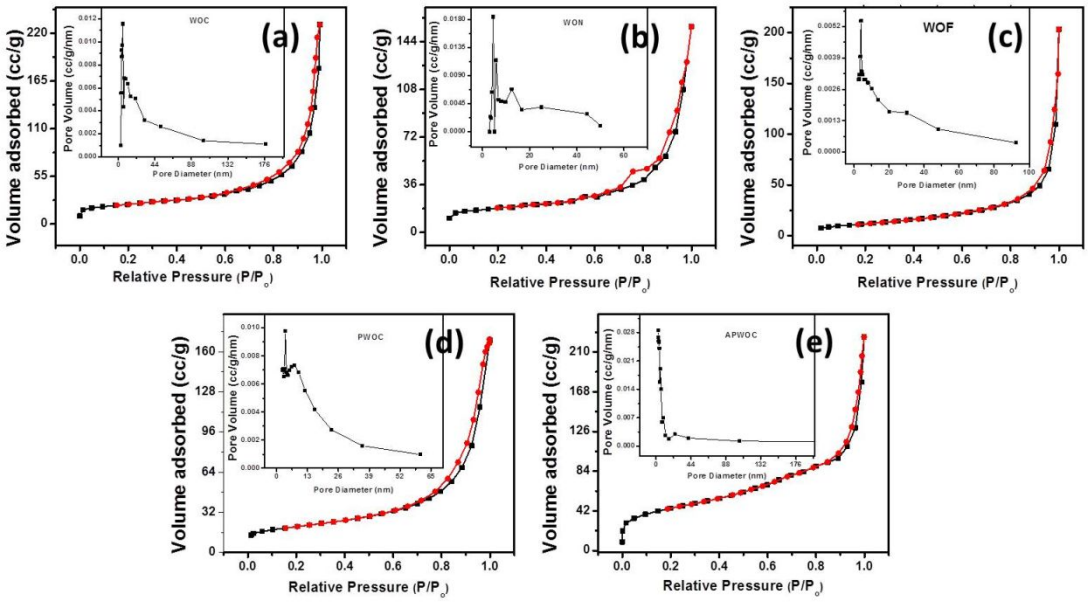

Figure S3. Nitrogen (N_2) adsorption–desorption curves of Cu-doped (a), Ni-doped (b), and Fe-doped $K_2W_4O_{13}$ (c) and PdO modified Cu-doped $K_2W_4O_{13}$(e), AuPdO modified Cu-doped $K_2W_4O_{13}$(e). Inset figures show pore size distribution curves for different morphologies of WO_3 nanowires.

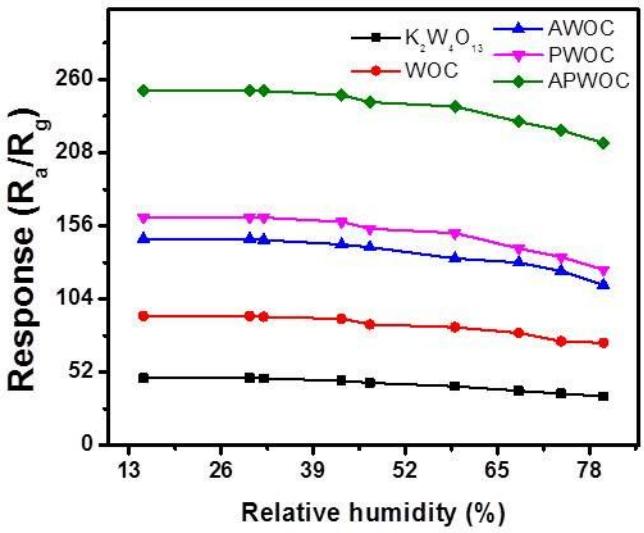

Figure S4. The sensor responses variation under relative humidity of 15, 30, 47, 62, 76% RH with 10 ppm *3H-2B.*

References

1. Shang, Y.; Shi, R.; Cui, Y.; Che, Q.; Wang, J.; Yang, P., Urchin-Like $WO_{2.72}$ Microspheres Decorated With Au and Pdo Nanoparticles for The Selective Detection of Trimethylamine. *ACS Appl Nano Mater* **2020,** *3* (6), 5554-5564.
2. Zeb, S.; Peng, X.; Shi, Y.; Su, J.; Sun, J.; Zhang, M.; Sun, G.; Nie, Y.; Cui, Y.; Jiang, X., Bimetal Au-Pd Decorated Hierarchical WO_3 Na/nowire Bundles for Gas Sensing Application. *Sens. Actuators B: Chem* **2021,** *334*, 129584.
3. Zeb, S.; Peng, X. J.; Yuan, G. Z.; Zhao, X. X.; Qin, C. Y.; Sun, G. X.; Nie, Y.; Cui, Y.; Jiang, X. C., Controllable Synthesis of Ultrathin WO_3 Nanotubes and Nanowires with Excellent Gas Sensing Performance. *Sensor Actuat B-Chem* **2020,** *305*, 127435.
4. Zeb, S.; Sun, G. X.; Nie, Y.; Cui, Y.; Jiang, X. C., Synthesis of Highly Oriented WO_3 Nanowire Bundles Decorated with Au for Gas Sensing Application. *Sens. Actuators B Chem.* **2020,** *321*, 128439.